*International Journal of Engineering & Technology*, 7 (4.39) (2018) 230-237

International Journal of Engineering & Technology

*Website: www.sciencepubco.com/index.php/IJET*

***Research paper***



# An Improvement Intended For Multiple Crack Diagnosis Adopting Combo Artificial Intelligence Technique

**Jajneswar Nanda [1]*, Layatitdev Das [2], D.R. Parhi [3]**

[1] *Department of Mechanical Engineering, SOA University, Bhubaneswar, Odisha, India*
[2] *Department of Mechanical Engineering, VSSUT, Burla, Odisha, India*
[3] *Department of Mechanical Engineering, N.I.T. Rourkela, Odisha, India*
**Corresponding author E-mail: jajneswarnanda@soa.ac.in*

## Abstract

**Abstract:** In the existing article, an innovative combination technique has been efficiently implemented to properly recognize the specific position and intensity of the transverse surface crack in a fixed-fixed shaft. The rod is suitably fixed on two modest bearings at both ends including axial and twisting load for the fixed angular arrangement in the longitudinal direction. The fluctuation parametric measure so as expected frequencies, mode shapes are interrogated in the proximity of two crack depths ($b_i$) with their specific locations ($L_i$) using stress intensity factor. Stress intensity factor is typically an objective function of compliance matrices. It is estimated as implementing one desired end of the shaft as the fixed bearings with the considerable help of an analytical method. The identical shaft is designed precisely to accurately determine the vibration signatures at respective vicinity using correctly an experimental procedure.
A developed methodology MANFIS-GA (an inverse technique) is implemented correctly to identify the proper position and intensity of possible crack from any one of the direct bearing. Complex MANFIS system consists precisely of four composed ANFIS layer. The possible input to every ANFIS step is adequately equipped with the first three fundamental frequencies along with their modal values. The standard output of the active ANFIS part prognosticates the interim crack positions and desired depths. The interim outputs from four ANFIS (MANFIS) are carefully taken as the specific inputs to the automated G.A. system. The outputs from the modern G.A. system are invariably final crack locations along with crack depths. The potency of the satisfactory MANFIS-GA results is authenticated by correlating the results with the experimental setup. By reasonably interpreting the possible outcomes, it is presumed that this recommended methodology is valid for online and time saving for fault analysis of the cracked structure.

***Keywords***: *Multiple cracked shaft, status monitoring, fundamental frequency, and modal values, MANFIS-GA.*

## 1. Introduction

In the modern scenario, correct diagnosis of crack becomes a prime interest for an advanced machine. It moves to avoid the potential failures and saves the subsistence cost. Advanced exposure of crack with its generation is a challenge to avoid failure. Due to developing resilient, the modern machinery interrogated many techniques to test parts before utilization. Mehrjoo et al. [1] presented the effect of Transverse edge crack by monitoring its thickness in the Euler-Bernoulli beam. The local stiffness of the cracked beam is calculated using rotational spring based on Bettie's theorem. The outcomes from both experimental and finite methods have examined with the present model. Khiem et al. [2] derived an explicit expression for forwarding & inverse problem of multiple cracked beams. A forward problem has analyzed the crack parameters whereas the inverse problem used to determine the mode shape. A fuzzy logic structure with an innovative windowpane for finding the crack parameters has expounded by Chandrasekhar et al. [3]. The effect of the change in frequency due to the change of material properties is studied and results are analyzed with a robust fuzzy logic system. A mathematical model formulated by Saridakis et al [4] for determining crack parameters such as position, depth and relative angle for two transverse cracks from fixed end of shaft along longitudinal direction. They calculated the compliance matrix using strain energy and theory of fracture mechanics for different crack angle. They have introduced fuzzy logic, neural network and genetic algorithm to decrease the computational rate without deterioration of competency. Determination of crack parameters using Genetic algorithms has been proposed by Mohammad et.al [5]. Eigen frequencies with crack location and depth obtained by the analytical method have been utilized the in G.A to monitor the possible changes in Eigen values of the structural beam. In An optimization, Both Binary and continuous genetic algorithms were utilized to get the best clarification of the results. Panigrahi et al. [6] has examined microscopic fatigue crack on a beam and developed an objective function using genetic algorithm and residual force. The outputs for crack parameters are validated using analytical results and obtained good approximation. Studies presented by Singh et.al [7] used transverse forces responses to identify crack exist in the shaft and measured their location. They applied the finite element technique and Timoshenko beam theory to procedures the vibration response. Beena et al. [8] developed a new algorithm model using continuum mechanics approach for detecting the fault of cantilever beam based on the fuzzy cognitive map. Haryanto et al. [9] have planned a computational technique for crack diagnosis of the damaged structure using the neural network. The change in deflection and strain reduces in stiffness of the structure. They have preferred that the stated methodology is a way to detect the crack parameter. The results have validated taking back-propagation of the neural network. They approved to be a better model than the

**Copyright © 2018 Authors. This is an open access article distributed under the Creative Commons Attribution License, which permits unrestricted use, distribution, and reproduction in any medium, provided the original work is properly cited.**

displacement method. Lekhy and Novak et al. [10] have introduced a scheme based on defect appearance by an artificial neural network (feed-forward multilayer network) in combination with stochastic analysis and designing the failure of the structure due to the reduction in stiffness. Structural failure in an axially vibrating rod due to natural frequency and ant resonant frequency have exposed by Dilena et al. [11] using Fourier coefficients. They proved the results of numerical simulations are in good agreement with the conducted experiment. Chomette et al. [12] carried a study to control and identify multiple transverse cracks for truss structure. After a methodical inquiry, they predicted the existence of multiple cracks introducing a new rational fraction polynomial algorithm and confirmed the same by combining both the crack orientation and crack parameters. Saeed et al. [13] have presented a unique Neural Network along with adaptive neuro-fuzzy interface system for identification of crack in the curvilinear beam with variations in pulsation response. They predicted that ANFIS is skilled in alerting crack identification in a better way with less percentage error than ANN. A suitable technique proposed by Trans et al. [14] to detect fault inside the induction motor. A data-driven structure based on Fourier-Bessel (FB) expansion has presented to use the transient signal. They used a particular class of neural network system (NNS) which has modified by Fuzzy ARTMAP (SFAM) to contribute lower training period in corresponding to NNS. The output of the projected model has varifired with the existing signals from a selection motor in a special situation. The modal response of a crack shaft in bending and torsion using flexibility functions have presented by Rubio et al. [15] on adding a close form polynomial expression. The authentication of the developed methodology is agreed with the finite element method and experimental technique.

## 2. Theoretical Analyses of Shaft

The primary frequencies and mode patterns of a fractured shaft (fixed-fixed) can be estimated near fracture mechanics, applying the strain energy and stress intensity factor. The mathematical formulation is below carefully presented.

### 2.1 Evaluation of Confined Flexibility of Damaged Shaft under Axial and Bending Load

Figure.1 signifies a multi-fractured shaft (fixed at both ends) of diameter D. Two surface cracks of depth b1 and b2 with locations L1 and L2 are presented from one of the fixed ends. The cracks are preceded by a coupling influence generating both in the transverse as well as in the longitudinal direction of the shaft. The shaft is constrained with axial load F1 and bending load F2 as shown in Figure. A local flexibility has interposed due to the presence of the cracks with the order of 2 x 2 matrixes.

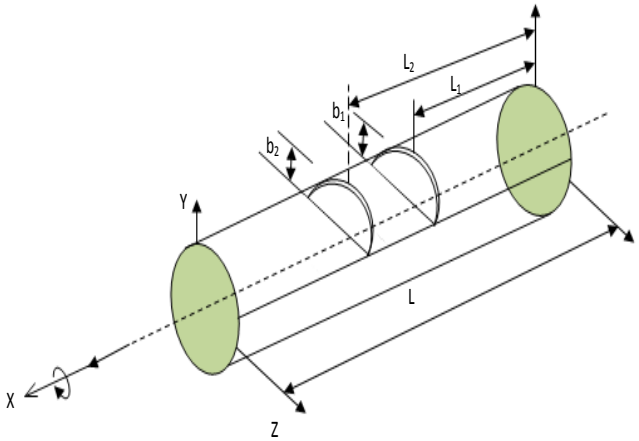


**Fig.1:** Shaft with multiple cracks

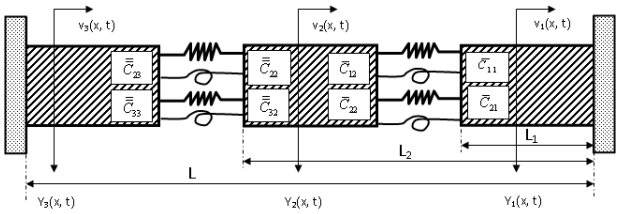


**Fig.2:** Crack Model

The strain energy release rate (Je) is obtained from stress intensity factor (Ci,j) at each fractured section using Fracture mechanics

$$J_e = \frac{1}{E'}\left(C_{11} + C_{12}\right)^2 \tag{1}$$

$$\frac{1}{E'} = \frac{1-\nu^2}{E} \text{ (Condition for plane strain)} \tag{1a}$$

$$\frac{1}{E'} = \frac{1}{E} \text{ (Condition for plane stress)} \tag{1b}$$

Poisson ratio (γ) Young's modules (Y) are the present values of the given specimen. Figure.2 represents the condition of displacements (vi) and stress intensity factors ($C_{i,\ j}$) for the opening of the cracks load $F_1$ and $F_2$ from one of the fixed end respectively. The experimental determined function is used to calculate values of compliance for two cracks using earlier studies. The stiffness matrix (Cij) is accomplished by accepting the inverse of compliance matrix $S_{i,j}$.

$$C = \begin{bmatrix} C_{11} & C_{12} \\ C_{21} & C_{22} \end{bmatrix} = \begin{bmatrix} S_{11} & S_{12} \\ S_{21} & S_{22} \end{bmatrix}^{-1} \tag{2}$$

The stiffness matrix for the first and second crack location (Figure 2) can be obtained using Equation 2.
1st crack location

$$\bar{C} = \begin{bmatrix} \bar{C}_{11} & \bar{C}_{12} \\ \bar{C}_{21} & \bar{C}_{22} \end{bmatrix} = \begin{bmatrix} \bar{S}_{11} & \bar{S}_{12} \\ \bar{S}_{21} & \bar{S}_{22} \end{bmatrix}^{-1} \tag{2a}$$

2nd crack location

$$\bar{\bar{C}} = \begin{bmatrix} \bar{\bar{C}}_{11} & \bar{\bar{C}}_{12} \\ \bar{\bar{C}}_{21} & \bar{\bar{C}}_{22} \end{bmatrix} = \begin{bmatrix} \bar{\bar{S}}_{11} & \bar{\bar{S}}_{12} \\ \bar{\bar{S}}_{21} & \bar{\bar{S}}_{22} \end{bmatrix}^{-1} \tag{2b}$$

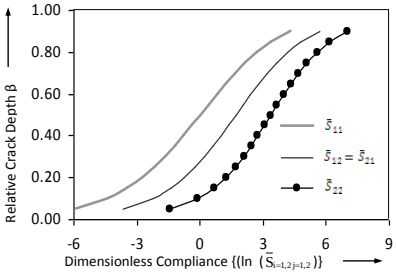


**Fig.3:** Relative Crack Depth (βi) vs. Dimensionless Compliance {(ln ¬ ( $\bar{S}_{i=1,2,\ j=1,2}$ )}

It is shown in Figure. 3 that the dimensionless acquiescence raises ($Si,j$) with rising relative crack depth ($\beta i$).

## 2.2. Analytical Calculation for Displacement of the Damaged Shaft

A cracked steel rod of length (L) bore (D) is presented in Figure 1. The rod has two surface cracks of different depths ($b_1$ and $b_2$). The cracks are used at a gap of $L_1$ and $L_2$ from the fixed end. The amplitudes of longitudinal vibration for the three parts (part 1, part 2, and part 3) are considered as $v_1(x, t)$, $v_2(x, t)$ and $v_3(x, t)$ respectively. Furthermore, the amplitude of bending vibration for the corresponding parts are $y_1(x, t)$, $y_2(x, t)$, $y_3(x, t)$ as given in Figure 2. The normal functions of the following crack parts for the given arrangement are represented in terms of ω, L, $C_v$.

$$\bar{v}_1(\bar{x}) = A_1 \cos(\bar{C}_v \bar{x}) + A_2 \sin(\bar{C}_v \bar{x}) \tag{3}$$

Similarly, for part 2 and part 3, the amplitudes of longitudinal vibration are $\bar{V}_2$, $\bar{V}_3$ respectively.

$$\bar{y}_1(\bar{x}) = A_7 \cosh(\bar{C}_y \bar{x}) + A_8 \sinh(\bar{C}_y \bar{x}) + A_9 \cos(\bar{C}_y \bar{x}) + A_{10} \sin(\bar{C}_y \bar{x}) \tag{4}$$

In a similarly way, for part 2 and part 3, the amplitudes of bending vibration for the respective sections are $\bar{y}_2$, $\bar{y}_3$ respectively.

All non-dimensional characters for properties of shafts are given as below.

$$\bar{x} = \frac{x}{L}, \bar{v} = \frac{v}{L}, \bar{y} = \frac{y}{L}, \alpha_1 = \frac{L_1}{L}, \ \alpha_2 = \frac{L_2}{L},$$

$$\bar{C}_v = \frac{\omega L}{C_v}, \bar{S}_v = \left(\frac{E}{\rho}\right)^{1/2}, \bar{C}_y = \left(\frac{\omega L^2}{S_y}\right)^{1/2}, S_y = \left(\frac{EI}{\mu}\right)^{1/2}, \mu = A\rho$$

Appling the end conditions for the fixed-fixed shaft, the constants ($A_{i=1to18}$) are to be determined.

The expression for crack section one ($L_1$) can be presented as given below.

$$\bar{v}_1'(\alpha_1) = \bar{v}_2'(\alpha_1); \quad \bar{y}_1(\alpha_1) = \bar{y}_2(\alpha_1);$$
$$\bar{y}_1''(\alpha_1) = \bar{y}_2''(\alpha_1); \quad \bar{y}_1''(\alpha_1) = \bar{y}_2'''(\alpha_1)$$
$$\bar{v}_1(0) = 0; \quad \bar{y}_1(0) = 0; \quad \bar{y}_1'(0) = 0$$
$$\bar{v}_1(1) = 0; \quad \bar{y}_1(1) = 0; \quad \bar{y}_1'(1) = 0$$
$$M_1 M_2 \bar{v}_1'(\alpha_1) = M_2(\bar{v}_2(\alpha_1) - \bar{v}_1(\alpha_1) + M_1(\bar{y}_2'(\alpha_1) - \bar{y}_1'(\alpha_1))$$
$$\bar{v}_2'(\alpha_2) = \bar{v}_3'(\alpha_2); \quad \bar{y}_2(\alpha_2) = \bar{y}_3(\alpha_2);$$
$$\bar{y}_2''(\alpha_2) = \bar{y}_3''(\alpha_2); \quad \bar{y}_2'''(\alpha_2) = \bar{y}_3'''(\alpha_2)$$

$$M_3 M_4 \bar{y}_1''(\alpha_1) = M_3(\bar{v}_2(\alpha_1) - \bar{v}_1(\alpha_1)) + M_4(\bar{y}_2'(\alpha_1) - \bar{y}_1'(\alpha_1)) \tag{5}$$

$$M_1 = \frac{AE}{LC_{11}}, M_2 = \frac{AE}{C_{12}}, \ M_3 = \frac{AI}{LC_{22}}, M_4 = \frac{EI}{L^2 C_{21}}$$

Similarly, the expression for first crack ($\alpha_2$) section can be presented as given below.

$$M_5 M_6 \bar{v}_2'(\alpha_2) = M_6(\bar{v}_3(\alpha_2) - \bar{v}_2(\alpha_2)) + M_5(\bar{y}_3'(\alpha_2) - \bar{y}_2'(\alpha_2)) \tag{6}$$

$$M_7 M_8 \bar{y}_2''(\alpha_2) = M_7(\bar{v}_3(\alpha_3) - \bar{v}_2(\beta_2)) + M_8(\bar{y}_3'(\alpha_2) - \bar{y}_2'(\alpha_2)) \tag{7}$$

Where, $M_5 = \frac{AE}{LC_{11}}, M_6 = \frac{AE}{C_{12}}, \ M_7 = \frac{EI}{LC_{22}}, M_8 = \frac{EI}{L^2 C_{21}}$

Equation (5) to Equation (7) all along the normal functions for the end conditions mentioned above, summarize to the appropriate equation for above the method is presented in Equation 8.

$$|Q| = 0 \tag{8}$$

This determinant is a function of natural frequency is ($\omega$), the relative crack location ($\alpha_1, \alpha_2$), relative crack depth ($\beta_1$ & $\beta_2$) and the local stiffness matrix ($C_{i,j}$).

The results of the theoretical analysis for the first three natural frequencies with two crack locations along with crack depths are shaft shown in Figure 4.

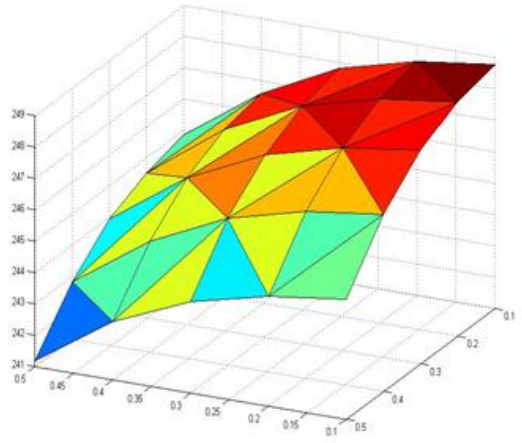

**Fig.4a:** (3rd Mode of vibration) Natural frequency of the cracked shaft vs. length from the fixed end L1/L =0.1…to.45, L2/L = 0.8, b1/D = 0.1…to0.5, b2/D = 0.2

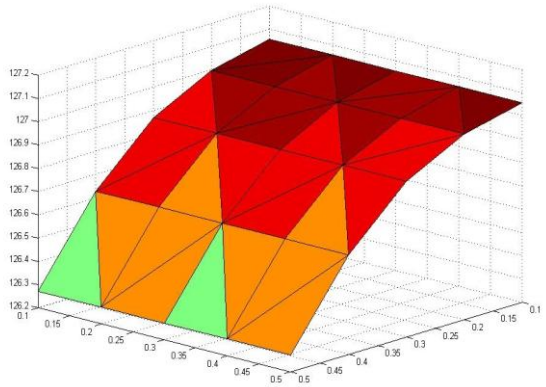

**Fig.4b:** (2nd Mode of vibration) Natural frequency of the cracked shaft vs. length from the fixed end L1/L =0.1…to.45, L2/L = 0.8, b1/D = 0.1…to0.5, b2/D = 0.2

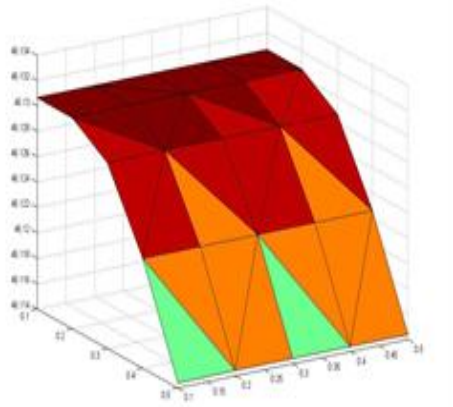

**Fig.4c:** (1st Mode of vibration) Natural frequency of the cracked shaft vs. length from the fixed end L1/L =0.1…to.45, L2/L = 0.8, b1/D = 0.1…to0.5, b2/D = 0.2

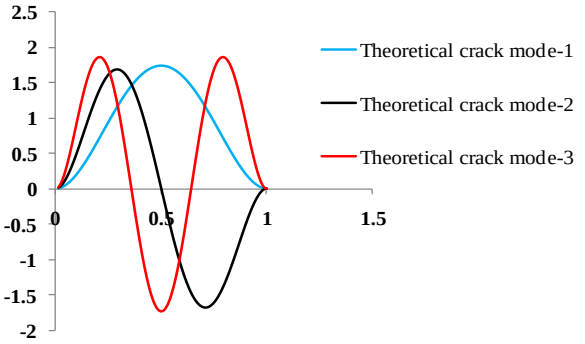


**Fig.5:** (All three Modes of vibration) Displacement of the cracked shaft vs. length from the fixed end L1/L =0.1, L2/L = 0.8, b1/D = 0.2, b2/D = 0.2

## 3. Experimental Set-Up

Test on the different specimen is conducted to identify the fundamental frequencies including mode patterns for various crack depths on steel shaft of length 1000mm and diameter 150mm. The laboratory set-up is presented in Figure 11. The amplitude of vibration at separate sections accompanying the length of the shaft is marked by putting the vibration pick-up and harmonizing the generator at the identical reverberating frequencies. The outcomes for the first three modes are outlined in Figure.12

1. Vibration pick-up
7. Power amplifier (Accelerometer)
2. Vibration Analyzer
8. Vibration Exciter (PULSE lite type 3560L)
3. Vibration indicator with
9. Cantilever beam Specimen
Software (PULSE lab shop software)
4. Distribution box
5. Power supply
6. Function Generator

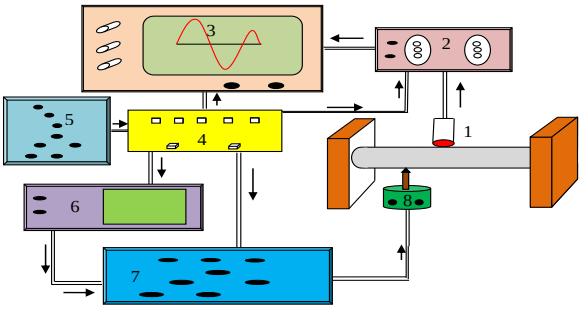

**Fig.11:** Experimental Setup

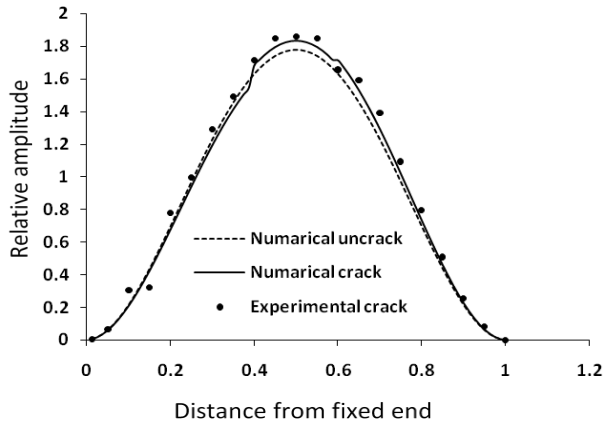


**Fig.11a:** Relative amplitude vs. distance from the fixed end (1st Mode of vibration) L1 =0.015m, L2 = 0.85m, b1/D = 0.2, b2/D = 0.6

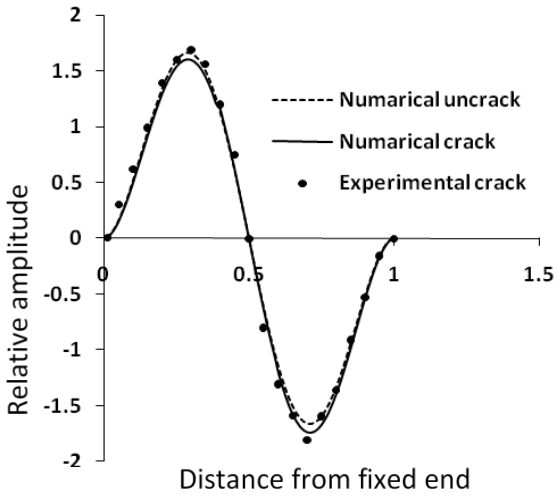


**Fig.11b:** Relative amplitude vs. distance from the fixed end (2nd Mode of vibration) L1 = 0.015m, L2 = 0.85m, b1/D = 0.2, b2/H = 0.6

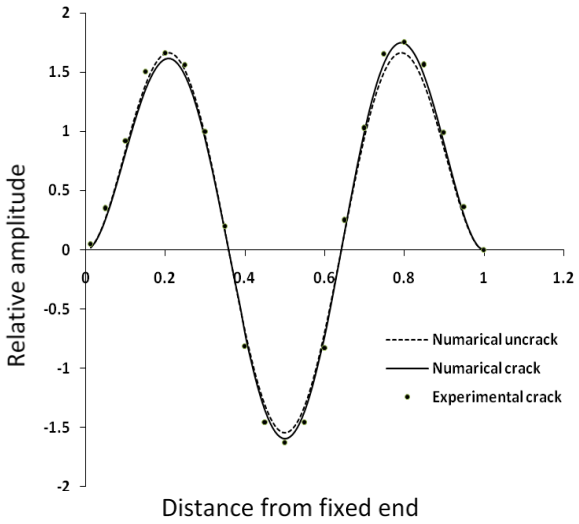


**Fig.11c:** Relative amplitude vs. distance from the fixed end (3rd Mode of vibration) L1 = 0.015 m, L2 = 0.85m, b1/D = 0.2, b2/D = 0.6

## 4. Analysis of Manfis for Detection of Multiple Cracks

### 4.1. Introduction to MANFIS

There are several method (non-destructive method) developed to identify the transverse multiple crack in the shaft or beam before catastrophic failure. Neural network, fuzzy-logic, genetic algorithm are some useful reverse technique applied for fault analysis of a damage structure. The present article represents a reversed method using multiple adaptive neuro-fuzzy evolutionary methods (MANFIS) to recognize multiple transverse cracks in the steel shaft fixed at both ends. The new technique known as MANFIS is one of the advance method based on the fuzzy-logic and neural system which integrate the positive features of both techniques. The advantage of using the newly developed technique for prediction of crack inaccurate position and depth is a great achievement for research analysis.

### 4.2 Steps to MANFIS

The multiple works of ANFIS from a new hybrid system is known as MANFIS. ANFIS controller consists of five layers as presented in Figure. 8. The first input layer of ANFIS designed in the basic principle of Fuzzy inference system (adaptive layer) which accepts

six input parameters so as the prime three fundamental frequencies including their mode patterns obtained from theoretical analysis. The input layer is with different Fuzzy logistics terms and several Fuzzy rules.

Both subsequent 2nd and 3rd layer are called unchanging layer. The 4th and 5th layers of ANFIS are also called adaptive layers. The interim results obtain from fifth layer of ANFIS are crack position and crack depth as shown in Figure.7. The output of MANFIS system are $N_{5,1,1\ (interim,}$ $N_{5,1,2\ (interim),}$ $N_{5,1,3\ (interim),}$ $N_{5,1,4\ (interim)}$. This new technique is employed for non-linear and complex function. It is only an extended work of ANFIS to obtain several output from a given control system. In the system, four ANFIS have been employed to predict four interim results as shown in Figure.8. The results obtain from MANFIS controller is well in agreement with experimental results. Consequently, the existing advance procedure is one suitable technique for prognosticating the crack for all models of vibrating arrangement.

### 4.3 Analysis for Crack Detection using Multiple Adaptive Neuro-fuzzy Inference Method

Four number of ANFIS group mutually to form MANFIS. The controller of ANFIS is employed for designing the controller of MANFIS. In the existing scenario, six parameters for the shaft are utilized as data to the MANFIS method and four variables are worked for products from the model. The input parameters of the shaft are inf ($x_1$), mnf ($x_2$), fnf ($x_3$), amd ($x_4$), bmd ($x_5$) and cmd ($x_6$). The output parameters of shaft are as follows; primary relative crack location $N_{5,\ 1,\ 1\ (interim)}$); primary relative crack depth $N_{5,\ 1,\ 2\ (interim)}$ secondary relative crack location $N_{5,\ 1,\ 3\ (interim);}$ secondary relative crack depth $N_{5,\ 1,\ 4\ (interim).}$ The yield parameter collected by MANFIS is based on following the logistic system.

The percentage change in fundamental natural frequency can be estimated as given below.

% Change in natural frequency

$$(inf,mnf,fnf)_i = \left| \frac{f_i^{uncracked} - f_i^{cracked}}{f_i^{uncracked}} \right| x100 \qquad (9)$$

Similarly the % Change in mode shape $(amd,bmd,cmd)_i$ =

$$\left| \frac{y_i^{uncracked} - y_i^{cracked}}{y_i^{uncracked}} \right| x100 \qquad (10)$$

$Y_i$ represents average mode shape difference for a given crack.

**Nominal rules for used MANFIS controller:**

Suppose $\Delta_I$ (i=1 to 6) be the fuzzy memberships shades fixed for the input variable $x_1$ to $x_6$ and $p_1$ to $p_6$. These are fuzzy membership function for the inputs variable. The policy for the MANFIS system are fixed as follows given in the Equation 9.

If $x_1$ is $(\Delta_1)_f$, $x_2$ is $(\Delta_2)_g$, $x_3$ is $(\Delta_3)_h$, $x_4$ is $(\Delta_4)_j$, $x_5$ is $(\Delta_5)_k$, $x_6$ is $(\Delta_6)_m$
Then
$F_{e,i} = q_{e,i}\, x_1 + r_{e,i}\, x_2 + s_{e,i}\, x_3 + t_{e,i}\, x_4 + u_{e,i}\, x_5 + v_{e,i}\, x_6 + z_{e,i}$ (11)

For opening crack position ($L_1$/L), opening crack depth ($b_1$/D), subsequent crack location ($L_2$/L) and crack depths ($b_2$/D) are obtained for e=1 to 4, f = 1 to $p_1$; g = 1 to $p_2$; h = 1 to $p_3$; j = 1 to $p_4$; k = 1 to $p_5$ and m = 1 to $p_6$ and i = 1 to 5

The nodes present in a given layer of ANFIS model represent the similar functions. The results obtained from the output of one layer of ANFIS model is provided to input results for subsequent layer and show on.

**Layer 1:** Each node in the 1st layer is taken as rectangular load (adaptive node) Figure. 8 characterize by fuzzy membership function representing the degree to which inputs satisfy the quantifier. For six input parameters, the outputs obtained from consequent nodes are governed by the Equation.12.

$N_{1,\ g,e} = \square\square\Delta_1)_g\,(x)$ for g = 1, ……, $p_1$,for input $x_1$ (12)

Similarly, other input such as $x_2$, $x_3$, $x_4$, $x_5$, and $x_6$ can be find out taking g = $p_1$+1and so on.

The Bell-shaped membership function ($\Delta$) is considered to get better output as given in the Figure.6.

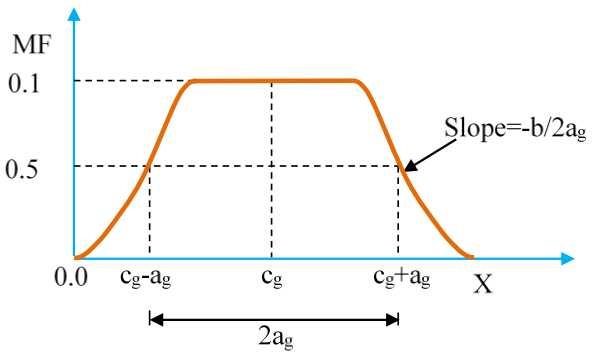


**Fig.6:** Bell-shaped (Membership function)

$$m(\Delta_i)_g(x_i) = \frac{1}{1+\left\{\left(\frac{x-c_g}{a_g}\right)^2\right\}^{b\,g}}; g = 1,\ \ldots\ldots,\ p_1 \qquad (13)$$

The parameters for the fuzzy membership function are $a_g$, $b_g$ and $c_g$. The value of $a_g$ $b_g$ and $c_g$ will change depending upon input parameters ($x_i$) of the shaft.

**Layer 2:** It is a fixed layer. The output obtained from the second layer is presented by $N_{2,\ i,\ e}$. The output is result of all received gesture.

$N_{2,i,e} = w_{i\ ,e} = \square\square\Delta_1)_g\,(x)\ \square\square\Delta_2)_g\,(x)\ \square\square\Delta_3)_g\,(x)\ \square\square\Delta_4)_g\,(x)\ \square\square\Delta_5)_g(x)\ \square\square\Delta_6)_g(x)$; (14)

For i = one to $p_i$ (i=1 to 5) and g = one… $p_1$+$p_2$+$p_3$+$p_4$+$p_5$+$p_6$ and $W_{I,\ e}$ is called the firing strength.

**Layer 3:** The node represents in third layer is fixed and the third layer output is estimated by the ratio of firing potentiality using the rule ($w_{i,e}$).

$$N3,\ i,\ e = \bar{w}_{i,e} = \frac{w_{i,e}}{\sum_{r-1}^{r=p_1\cdot p_2\cdot p_3\cdot p_4\cdot p_5\cdot p_6} w_{r,e}} \qquad (15)$$

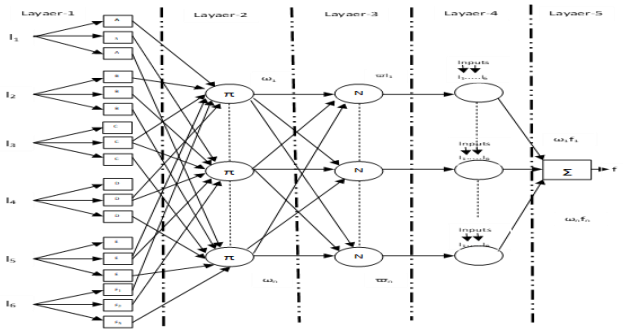


**Fig.7:** Multi crack detection using Adaptive-Neuro-Fuzzy-Inference structure

**Layer 4:** The fourth level is adaptive layer and represented with a node N4,i, e

$$N_{4,i,e} = \bar{w}_{i,e} \quad F_{e,i} = \bar{w}_{i,e} (Q_{e,i} X_1 + R_{e,i} X_2 + S_{e,i} X_3 + T_{e,i} X_4 + U_{e,i} X_5 + V_{e,i} X_6 + Z_{e,I}) \quad (16)$$

$\bar{w}_{i,e}$ is the standard firing strength form (output) of third layer Qe,i , Re,i , Se,i , Te,i, Ue,i , Ve,i , Ze,i are the set of parameters for crack location and depth.

**Layer 5:** The particular layer in this node is fixed node layer .The result received from fifth level is taken as cumulative of all received signals.

$$N_{5,1,e} = \sum_{i-1}^{i=P_1.P_2.P_3.P_4.P_5.P_6} W_{i,e} F_{e,i} = \frac{\sum_{i-1}^{i=P_1.P_2.P_3.P_4.P_5.P_6} W_{i,e} F_{e,i}}{\sum_{i-1}^{i=P_1.P_2.P_3.P_4.P_5.P_6} W_{i,e}} \quad (17)$$

In the existing ANFIS arrangement, six-dimensional extents contributed to six-shaft designs parameter designated by $P_1$ x $P_2$ x $P_3$ x $P_4$ x $P_5$ x $P_6$ range. Every section is ruled by the fuzzy technique. The regressive pass error signals generate backward, begin the parameter, and refreshed it by gradient descent technique. The MANFIS designs are exhibited in Figure 8.

### 4.4 Results of MANFIS

The simulation outcomes in the modern study are to prognosticate the crack positions and depths. The outcomes are accepted as the base for the formulation of a crack diagnosis tool utilizing the procedure. The bell shaped function is adopted for intending the ANFIS model. Outputs in expressions of corresponding crack position and depths are presented in form of interim results such as $N_{5,1,1\ (interim}$ , $N_{5,1,2\ (interim)}$, $N_{5,1,3\ (interim)}$, and $N_{5,1,4\ (interim)}$ The agreement of the MANFIS system has been validated by correlating the outcomes with the experimental study in later part.

### 4.5 Crack Characteristic Tool using GA

### 4.5.1 Using the Principle of GA

Genetic algorithm is a method based on genetics and used to optimize large number of variable with non-linear scatter data. Hence, GA has greater importance in solving complicated problem than any other method. The present methodology predicts the position of crack with its depth taking ten input parameters such as inf, mnf, fnf, amd, bmd, cmd from analytical and four interim results of MANFIS. On utilizing these chromosomes, GA controller generates hundreds of chromosomes, which represent as the parents. These values act like chromosome for GA and present like data pool. The systematic procedure for obtaining crack location and crack depth are as follows.

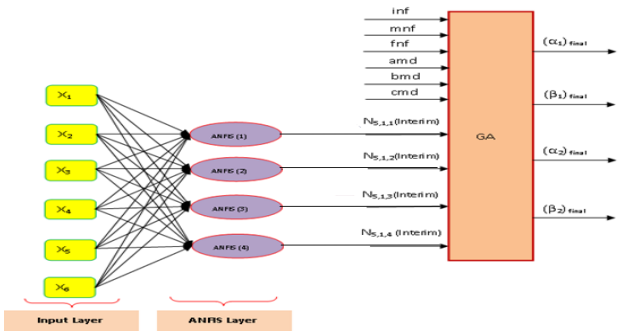


**Fig.8:** MANFIS-GA System for crack detection

**Stage 1: To create an objective function**

GA based methodology is to formulate an objective function which is both quantified and minimized to provide best results for a given population. In the present problem, the genes variables that act as chromosomes are ten in numbers. They are three relative natural frequency inf, mnf, fnf, three relative mode shape difference amd ,bmd, cmd, $N_{5,1,1\ (interim,}$ $N_{5,1,2\ (interim),}$ $N_{5,1,3\ (interim),}$ $N_{5,1,4\ (interim),}$

Chromosome= [inf, mnf, fnf, amd, bmd, cmd, $N_{5,1,1\ (interim,}$ $N_{5,1,2\ (interim),}$ $N_{5,1,3\ (interim),}$ $N_{5,1,4\ interim)}$]

The specific function can be formulated as Z $\{(\alpha_1)_{final,} (\beta_1)_{final,} (\alpha_2)_{final,} (\beta_2)_{final}\}$

$$= \{(\inf_p - \inf_{x_1,i})^2 + (mnf_p - mnf_{x_1,i})^2 + (fnf_p - fnf_{x_1,i})^2 + (amd_p - amd_{x_1,i})^2 + (amd_p - amd_{x_1,i})^2 + (bmd_p - bmd_{x_1,i})^2 + (cmd_p - cmd_{x_1,i})^2 + [(N_{5,i,e})_p - \alpha_{x_1,i}]^2 + [(N_{5,i,e})_p - \beta_{x_1,i}]^2 + [(N_{5,i,e})_p - \alpha_{x_2,i}]^2 + [(N_{5,i,e})_p - \beta_{x_2,i}]^2\}^{0.5} \quad (18)$$

Fundamental frequencies along with modal values of the population for first second and third are $inf_p$, $mnf_p$, $fnf_p$, $amd_p$, $bmd_p$, $cmd_p$.

Fundamental frequencies along with mode values of the theoretical analysis for first, second and third are $inf_x$,$mnf_x$,$fmf_x$, $amd_x$, $bmd_x$, $cmd_x$

Crack positions and depths for the population obtain from MANFIS (for $i,e=1$ to 4) is $N_{5,i,e}$. Usual crack locations and depths are $\alpha_{X\,i}$, βx,I for iterations ( $i=$ 1 to i=n) The smallest volume of objective function will give the optimal solution from the given population.

**Stage 2: Accumulation of data in Data pool:**

The original input supply of proposed size is created including hundreds of calculated data using the objective function. Every original data set of the generated data supply signifies the chromosomes of that GA model. Within this research, generated characters from the set are the search space for the problem. The original population including dimension n is displayed.

Original Population = <$Q_1$, $Q_2$… Qn>

Every formation has the components $Q_{i,j}$, which are commonly an integer starting of range L.Every group segments maintain 10-sets of genes which are designated by character numerals 1 to 10. $Q_i = \{q_{1,1} q_{1,2}\ q_{1,3}\ q_{1,4}\ q_{1,5}\ q_{1,6}\ q_{1,7} q_{1,8}\ \ q_{1,9}\ q_{1,10}\}$ (20)

Similarly, $Q_n$ can be presented. The element No. 1 ($q_{1,1}$ to $q_{n,1}$) to element No. 10 represent original frequencies, mode patterns, crack positions and crack depths obtained from the theoretical analysis are used to train the GA based controller for prediction of cracks in damaged structures.

**Stage 3: Choice of the best-fit chromosome for reproduction**

To get the optimal decision, the GA process the information (population data) generate product for the second stage. The product parameters are correlated amidst the chromosomes of the original input and the best-fit chromosome is chosen to be an optimal resolution. Approximately, best-fit chromosomes are chosen to be parents for generation rejecting the excess of the chromosomes inside the group.

**Stage 4: Investigation of crossover and mutation**

Genes present in the chromosomes are encoded to binary bits for crossover operation. In our work each gene contain ten bits, thus each chromosome contain hundred bits. The crossover operation has been used in the present research to increase reproduction population of the data pool. Some of the examples of crossover method are presented within Figure. 9.

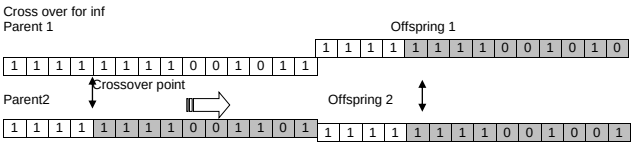


**Fig.9:** Single cross point, value encoding

Crossover for inf, mnf, fnf, amd, bmd, cmd, $(\alpha_1)$ final, $(\beta_1)$ final, $(\alpha_2)$ final, $(\beta_2)$ final

The sequence of genes can be generated by changing the binary code in the Mutation process. The robustness regarding the chromosome among the reduced genes is estimated for deciding the optimal interpretation. If the consistency of the mutated chromosome is greater than the overall population, that will persevere and possibly be permitted to mate among different chromosomes. Few of the examples obtained from the mutation operation are represented below in Figure.10

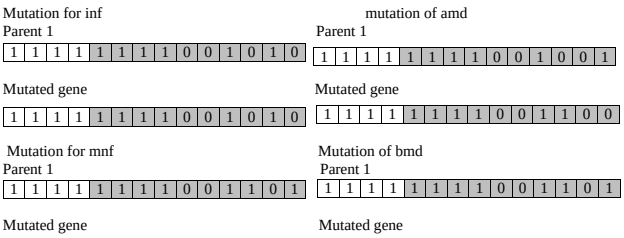


**Fig.10:** Mutations of genes for inf, mnf, fnf, amd, bmd, cmd

### Stage 5: Estimation of the appropriate child

The mutation and crossover method create unique chromosomes by recently formed genes. These unique chromosomes are judged to determine the final solution. The crossover and the recently created chromosome from the mutation method are correlated with the outcomes from the information supply to obtain the strongest child.

The evaluation of the appropriate child is estimated as given below.

**Objective functions**

$$\{(\alpha_1)\,final,\ (\beta_1)\,final,\ (\alpha_2)\,final,\ (\beta_2)\,final)\} =$$

$$\{(\inf_{fld} - \inf_{x_1,i})^2 + (\mathrm{mnf}_{fld} - m\mathrm{nf}_{x_1,i})^2 + (\mathrm{fnf}_{fld} - fnf_{x_1,i})^2\}^{0.5} +$$
$$\{(\mathrm{amd}_{fld} - amd_{x_1,i})^2 + (\mathrm{bmd}_{fld} - bmd_{x_1,i})^2 + (\mathrm{cmd}_{fld} - cmd_{x_1,i})^2\}^{0.5} +$$
$$\{[(\alpha_1)_{fld} - \alpha_{x_1,i}]^2 + [(\beta_1)_{fld} - \beta_{x_1,i}]^2 + [(\alpha_2)_{fld} - \alpha_{x_2,i}]^2 + [(\beta_2)_{fld} - \beta_{x_2,i}]^2\}^{0.5} \quad (21)$$

The recommended genetic algorithm model has ten inputs data with four outputs. The final crack locations and depths for multi crack shaft are $(\alpha_1)$ final, $(\beta_1)$ final, $(\alpha_2)$ final, $(\beta_2)$ final

For better understanding of the method the training and testing input data for MANFIS-GA network is presented in Table 1.

**Table 1:** Training and testing input data for MANFIS-GA network for fixed-fixed shaft

| Output | | | | | | | |
|---|---|---|---|---|---|---|---|
| Test values (Experimental results) | | | | Test values (MANFIS- GA) results | | | |
| $\alpha_{e,1}$ | $\beta_{e,1}$ | $\alpha_{e,2}$ | $\beta_{e,2}$ | $\alpha_1$ | $\beta_1$ | $\alpha_2$ | $\beta_2$ |
| 0.10 | 0.10 | 0.80 | 0.10 | 0.0981 | 0.0978 | 0.7797 | 0.0982 |
| 0.10 | 0.10 | 0.80 | 0.30 | 0.0978 | 0.1008 | 0.7802 | 0.2942 |
| 0.10 | 0.10 | 0.80 | 0.50 | 0.0988 | 0.0978 | 0.7799 | 0.4930 |
| 0.10 | 0.30 | 0.80 | 0.10 | 0.0972 | 0.2932 | 0.7798 | 0.0981 |
| 0.10 | 0.30 | 0.80 | 0.30 | 0.0991 | 0.2931 | 0.7795 | 0.2932 |
| 0.10 | 0.30 | 0.80 | 0.50 | 0.0990 | 0.3035 | 0.7794 | 0.4957 |
| 0.10 | 0.50 | 0.80 | 0.10 | 0.0981 | 0.4904 | 0.7800 | 0.0982 |
| 0.10 | 0.50 | 0.80 | 0.30 | 0.0983 | 0.4890 | 0.7796 | 0.2928 |
| 0.10 | 0.50 | 0.80 | 0.50 | 0.0978 | 0.4907 | 0.7793 | 0.4909 |
| 0.35 | 0.10 | 0.65 | 0.10 | 0.3422 | 0.0984 | 0.6482 | 0.0979 |
| 0.35 | 0.10 | 0.65 | 0.30 | 0.3424 | 0.0997 | 0.6404 | 0.2935 |
| 0.35 | 0.10 | 0.65 | 0.50 | 0.3428 | 0.0988 | 0.6408 | 0.4958 |
| 0.35 | 0.30 | 0.65 | 0.10 | 0.3432 | 0.2937 | 0.6423 | 0.0982 |
| 0.35 | 0.30 | 0.65 | 0.30 | 0.3435 | 0.2935 | 0.6440 | 0.2938 |
| 0.35 | 0.30 | 0.65 | 0.50 | 0.3427 | 0.3024 | 0.6373 | 0.4957 |
| 0.35 | 0.50 | 0.65 | 0.10 | 0.3429 | 0.4915 | 0.6381 | 0.0980 |
| 0.35 | 0.50 | 0.65 | 0.30 | 0.3439 | 0.4949 | 0.6384 | 0.2937 |
| 0.35 | 0.50 | 0.65 | 0.50 | 0.3430 | 0.4910 | 0.6332 | 0.4957 |
| 0.45 | 0.10 | 0.55 | 0.10 | 0.4408 | 0.0990 | 0.5550 | 0.0981 |
| 0.45 | 0.10 | 0.55 | 0.30 | 0.4410 | 0.0993 | 0.5358 | 0.2925 |
| 0.45 | 0.10 | 0.55 | 0.50 | 0.4416 | 0.1001 | 0.5357 | 0.4955 |
| 0.45 | 0.30 | 0.55 | 0.10 | 0.4448 | 0.2933 | 0.5358 | 0.0984 |
| 0.45 | 0.30 | 0.55 | 0.30 | 0.4422 | 0.2926 | 0.5369 | 0.2926 |
| 0.45 | 0.30 | 0.55 | 0.50 | 0.4435 | 0.2927 | 0.5369 | 0.4930 |
| 0.45 | 0.50 | 0.55 | 0.10 | 0.4419 | 0.4888 | 0.5353 | 0.0979 |
| 0.45 | 0.50 | 0.55 | 0.30 | 0.4445 | 0.4874 | 0.5364 | 0.2928 |
| 0.45 | 0.50 | 0.55 | 0.50 | 0.4443 | 0.4875 | 0.5357 | 0.4906 |

$\alpha_{e,i}$,$\beta_{e,i}$ : Experimental location and depth: $(\alpha_i)_f$, $(\beta_i)_f$ :GA-MANFIS model location and depth for fixed-fixed shaft;

## 5. Discussions

From the review of the results received from the various methods for crack investigation in the present paper, it is commented that the appearance of cracks at the structure Figure.1 has an ample influence on its vibration response. The changes of dimensionless compliance including the crack depth have given in Figure. 3. The results of fractures on the first three mode shapes of the shaft have shown in Figure 4 and 5. An experimental study for the fractured shaft displayed with the provided set up is shown in Figure. 11. The vibration responses received from the analytical and experimental study are utilized to outline the MANFIS model for the hybrid system. The methodology has been shown in Figure.7 and Figure. 8 individually. Table 1 represents the training and testing input data of MANFIS-GA for Fixed-Fixed shaft. The MANFIS-GA method has been examined by error report taking the Equation 22 with relating to experimental analysis. A correlation of results from experimental analysis with MANFIS-GA mode is presented in Table 2.

$$\text{Percentage of deviation} = \frac{\left|\text{Experimental crack location/depth Fixed-Fixed shaft} - \text{GA-MANFIS model based crack location/depth Fixed-Fixed shaft}\right|}{\text{Experimental crack location/depth Fixed-Fixed shaft}} \times 100 \quad (22)$$

**Table 2:** Comparison of % errors in GA-MANFIS vs. test values for fixed-fixed shaft

| Input data | | | | | | | | | | | | Output data | | | | | | | | |
|---|---|---|---|---|---|---|---|---|---|---|---|---|---|---|---|---|---|---|---|---|
| Sl. No | Test points(Experimental) | | | | % change in natural frequency | | % change in maximum mode shape | | | MANFIS-GA | | | | %(MANFIS-GA) error | | | | | | |
| | $\alpha_{e,1}$ | $\beta_{e,1}$ | $\alpha_{e,2}$ | $\beta_{e,2}$ | inf | mnf | fnf | amd | bmd | cmd | $(\alpha_1)_{final}$ | $(\beta_1)_{final}$ | $(\alpha_2)_{final}$ | $(\beta_2)_{final}$ | % error in $(\alpha_1)_{final}$ | % error in $(\beta_1)_{final}$ | % error in $(\alpha_2)_{final}$ | % error in $(\beta_2)_{final}$ | | |
| 1 | 0.10 | 0.20 | 0.80 | 0.20 | 0.2736 | 0.1259 | 0.1475 | 0.0403 | 0.1207 | 0.2798 | 0.0979 | 0.1997 | 0.7867 | 0.1976 | 2.0962 | 0.1501 | 1.6608 | 1.1980 | | |
| 2 | 0.15 | 0.20 | 0.75 | 0.20 | 0.2306 | 0.0821 | 0.1859 | 0.0174 | 0.1484 | 0.0888 | 0.1457 | 0.1966 | 0.7375 | 0.1966 | 2.8613 | 1.6970 | 1.6709 | 1.6970 | | |
| 3 | 0.20 | 0.20 | 0.70 | 0.20 | 0.1914 | 0.0922 | 0.2607 | 0.0035 | 0.1280 | 0.1746 | 0.1946 | 0.1971 | 0.6879 | 0.1977 | 2.6950 | 1.4475 | 1.7258 | 1.1481 | | |
| 4 | 0.25 | 0.20 | 0.65 | 0.20 | 0.1634 | 0.1390 | 0.2955 | 0.0210 | 0.0605 | 0.3525 | 0.2445 | 0.1956 | 0.6406 | 0.1946 | 2.1960 | 2.1960 | 1.4469 | 2.6950 | | |
| 5 | 0.30 | 0.20 | 0.60 | 0.20 | 0.1364 | 0.1977 | 0.2514 | 0.0348 | 0.0354 | 0.3203 | 0.2924 | 0.1946 | 0.5917 | 0.2007 | 2.5287 | 2.6950 | 1.3911 | 0.3489 | | |
| 6 | 0.35 | 0.20 | 0.55 | 0.20 | 0.1212 | 0.2642 | 0.1639 | 0.0460 | 0.1325 | 0.1253 | 0.3433 | 0.1945 | 0.5433 | 0.1959 | 1.9109 | 2.7449 | 1.2150 | 2.0463 | | |
| 7 | 0.40 | 0.20 | 0.50 | 0.20 | 0.1087 | 0.3044 | 0.0713 | 0.0514 | 0.1999 | 0.1037 | 0.3902 | 0.1959 | 0.4931 | 0.1965 | 2.4455 | 2.0463 | 1.3878 | 1.7469 | | |
| 8 | 0.10 | 0.30 | 0.80 | 0.30 | 0.7790 | 0.3694 | 0.4257 | 0.1132 | 0.3290 | 0.7616 | 0.0980 | 0.2934 | 0.7878 | 0.2938 | 1.9964 | 2.1960 | 1.5218 | 2.0629 | | |
| 9 | 0.15 | 0.30 | 0.75 | 0.30 | 0.6688 | 0.2618 | 0.5517 | 0.0510 | 0.4157 | 0.2468 | 0.1457 | 0.2955 | 0.7396 | 0.2937 | 2.8613 | 1.4974 | 1.3878 | 2.0962 | | |
| 10 | 0.20 | 0.30 | 0.70 | 0.30 | 0.5695 | 0.2863 | 0.7447 | 0.0056 | 0.3535 | 0.4879 | 0.1987 | 0.2917 | 0.6899 | 0.2933 | 0.6491 | 2.7615 | 1.4369 | 2.2293 | | |
| 11 | 0.25 | 0.30 | 0.65 | 0.30 | 0.4842 | 0.4127 | 0.8360 | 0.0551 | 0.1662 | 0.9691 | 0.2424 | 0.2928 | 0.6414 | 0.2937 | 3.0343 | 2.3956 | 1.3224 | 2.0962 | | |
| 12 | 0.30 | 0.30 | 0.60 | 0.30 | 0.4100 | 0.5846 | 0.7216 | 0.0940 | 0.0943 | 0.8946 | 0.2913 | 0.2961 | 0.5911 | 0.2941 | 2.8946 | 1.2978 | 1.4754 | 1.9631 | | |
| 13 | 0.35 | 0.30 | 0.55 | 0.30 | 0.3677 | 0.7586 | 0.4777 | 0.1243 | 0.3625 | 0.3533 | 0.3444 | 0.2950 | 0.5419 | 0.2938 | 1.5972 | 1.6637 | 1.4723 | 2.0629 | | |
| 14 | 0.40 | 0.30 | 0.50 | 0.30 | 0.3403 | 0.8905 | 0.2238 | 0.1440 | 0.5613 | 0.2835 | 0.3922 | 0.2962 | 0.4916 | 0.2934 | 1.9465 | 1.2645 | 1.6709 | 2.1960 | | |
| 15 | 0.10 | 0.40 | 0.80 | 0.40 | 0.1457 | 0.7980 | 0.9289 | 0.2412 | 0.7068 | 1.6207 | 0.0980 | 0.3928 | 0.7879 | 0.3916 | 1.9964 | 1.7968 | 1.5091 | 2.0962 | | |
| 16 | 0.15 | 0.40 | 0.75 | 0.40 | 0.1436 | 0.5818 | 1.2020 | 0.1076 | 0.8966 | 0.5133 | 0.1477 | 0.3917 | 0.7397 | 0.3914 | 1.5307 | 2.0713 | 1.3743 | 2.1461 | | |
| 17 | 0.20 | 0.40 | 0.70 | 0.40 | 0.1283 | 0.6248 | 1.5694 | 0.0104 | 0.7478 | 1.0347 | 0.1987 | 0.3918 | 0.6901 | 0.3912 | 0.6491 | 2.0463 | 1.4080 | 2.1960 | | |
| 18 | 0.25 | 0.40 | 0.65 | 0.40 | 1.0533 | 0.8941 | 1.7761 | 0.1164 | 0.3537 | 2.0414 | 0.2455 | 0.3906 | 0.6414 | 0.3910 | 1.7968 | 2.3457 | 1.3224 | 2.2459 | | |
| 19 | 0.30 | 0.40 | 0.60 | 0.40 | 0.9145 | 1.2626 | 1.5742 | 0.2033 | 0.2087 | 1.9079 | 0.2924 | 0.3904 | 0.5912 | 0.3915 | 2.5287 | 2.3956 | 1.4586 | 2.1212 | | |
| 20 | 0.35 | 0.40 | 0.55 | 0.40 | 0.8015 | 1.6119 | 1.0309 | 0.2642 | 0.7613 | 0.7633 | 0.3454 | 0.3901 | 0.5426 | 0.3917 | 1.3121 | 2.4705 | 1.3437 | 2.0713 | | |
| 21 | 0.40 | 0.40 | 0.50 | 0.40 | 0.7437 | 1.8860 | 0.4887 | 0.3063 | 1.1783 | 0.5788 | 0.3902 | 0.3895 | 0.4941 | 0.3920 | 2.4455 | 2.6202 | 1.1855 | 1.9964 | | |
| 22 | 0.10 | 0.50 | 0.80 | 0.50 | 3.1375 | 1.4884 | 1.7630 | 0.4497 | 1.3284 | 3.0006 | 0.0999 | 0.4877 | 0.7877 | 0.4894 | 0.1002 | 2.4555 | 1.5344 | 2.1162 | | |
| 23 | 0.15 | 0.50 | 0.75 | 0.50 | 2.7029 | 1.0976 | 2.2174 | 0.2060 | 1.6608 | 0.8808 | 0.1488 | 0.4861 | 0.7396 | 0.4880 | 0.7988 | 2.7748 | 1.3878 | 2.3956 | | |
| 24 | 0.20 | 0.50 | 0.70 | 0.50 | 2.2853 | 1.2096 | 2.9169 | 0.0194 | 1.4154 | 1.9449 | 0.1997 | 0.4859 | 0.6901 | 0.4900 | 0.1501 | 2.8148 | 1.4080 | 1.9964 | | |
| 25 | 0.25 | 0.50 | 0.65 | 0.50 | 1.9637 | 1.6613 | 3.2328 | 0.2095 | 0.6491 | 3.6983 | 0.2455 | 0.4858 | 0.6410 | 0.4882 | 1.7968 | 2.8347 | 1.3847 | 2.3557 | | |
| 26 | 0.30 | 0.50 | 0.60 | 0.50 | 1.6936 | 2.3181 | 2.8782 | 0.3681 | 0.3691 | 3.4773 | 0.2893 | 0.4890 | 0.5905 | 0.4886 | 3.5599 | 2.1960 | 1.5765 | 2.2758 | | |
| 27 | 0.35 | 0.50 | 0.55 | 0.50 | 1.5252 | 2.9639 | 1.9435 | 0.4887 | 1.4026 | 1.4477 | 0.3413 | 0.4890 | 0.5421 | 0.4898 | 2.4811 | 2.1960 | 1.4356 | 2.0363 | | |

## 6. Conclusions

The results obtained from theoretical analyses are applied to artificial intelligence systems using hybrid MANFIS-GA. It is shown that the hybrid MANFIS-GA model produces a better result than that of Genetic algorithm and ANFIS with the best validation performance in case of Fixed-Fixed shaft. Correlating to the experimental database, the error is, within 1.69% and 1.77% for Fixed-Fixed shaft (crack location and depth). In overall, the common error in crack location and depth for all three-end conditions of the shaft using MANFIS-GA are 1.73%. The noble hybrid technique can be used on a diagnostic tool for accelerate prediction of crack location and crack depth in different structure. A good correspondence is recognized among the results of the experimental model and suggested MANFIS-GA model. In the current studies, the dynamic response of cracked and uncracked shaft for separate end conditions have been used for analysis and improvement by multiple crack diagnostic methods to provide a robust model for the condition monitoring of the dynamic structure.

## References


[1] M. Mehrjoo, N. Khaji, and M. Ghafory-Ashtiany, Application of genetic algorithm in crack detection of beam-like structures using a new cracked Euler–Bernoulli beam element, Applied Soft Computing, 13(2): p. 867-880, 2013.

[2] N. T. Khiem, and H. T. Tran, A procedure for multiple crack identification in beam-like structures from natural vibration mode, Journal of Vibration and Control, 20(9): p. 1417-1427, 2014.

[3] M. Chandrashekhar, and R. Ganguli, Uncertainty handling in structural damage detection using fuzzy logic and probabilistic simulation, Mechanical Systems and Signal Processing, 23(2): p.384-404, 2009.

[4] K. M. Saridakis, A. C. Chasalevris, C. A. Papadopoulos, and A. J. Dentsoras, Applying neural networks, genetic algorithms and fuzzy logic for the identification of cracks in shafts by using coupled response measurements, Computers & Structures, 86(11-12): p. 1318-1338, 2008.

[5] M. T. Vakil-Baghmisheh, M. Peimani, M. H. Sadeghi, and M. M. Ettefagh, Crack detection in beam-like structures using genetic algorithms, Applied soft computing, 8(2): p. 1150-1160, 2008.

[6] S. K. Panigrahi, S. Chakraverty, and B. K. Mishra, Vibration based damage detection in a uniform strength beam using genetic algorithm, Meccanica, 44(6): p. 697, 2009.

[7] S. K. Singh, and R. Tiwari, Identification of a multi-crack in a shaft system using transverse frequency response functions, Mechanism and machine theory, 45(12): p. 1813-1827, 2010.

[8] P. Beena, and R. Ganguli, Structural damage detection using fuzzy cognitive maps and Hebbian learning, Applied Soft Computing, 11(1): p. 1014-1020, 2011.

[9] I. Haryanto, J. D. Setiawan, and A. Budiyono, Structural damage detection using randomized trained neural networks. In Intelligent Unmanned Systems: Theory and Applications, Springer, Berlin, Heidelberg, p. 245-255, 2009.

[10] D. Lehký, and D. Novák, Neural network based damage detection of dynamically loaded structures, In International Conference on Engineering Applications of Neural Networks, Springer, Berlin, Heidelberg, p. 17-27, 2009.

[11] M. Dilena, and A. Morassi, Structural health monitoring of rods based on natural frequency and antiresonant frequency measurements, Structural health monitoring, 8(2): p. 149-173, 2009.

[12] B. Chomette, and J. J. Sinou, Crack detection based on optimal control, Journal of vibration and control, 18(11): p. 1737-1749, 2012.

[13] R. A. Saeed, A. N. Galybin, and V. Popov, Crack identification in curvilinear beams by using ANN and ANFIS based on natural frequencies and frequency response functions, Neural computing and applications, 21(7): p. 1629-1645, 2012.

[14] F. AlThobiani, A. Ball, and B. K. Choi, An application to transient current signal based induction motor fault diagnosis of Fourier–Bessel expansion and simplified fuzzy ARTMAP, Expert Systems with Applications, 40(13): p. 5372-5384, 2013.

[15] L. Rubio, B. Muñoz-Abella, and G. Loaiza, Static behaviour of a shaft with an elliptical crack, Mechanical Systems and Signal Processing, 25(5): p. 1674-1686, 2011.